THE JOURNAL OF BIOLOGICAL CHEMISTRY VOL. 281, NO. 42, pp. 31885–31893, October 20, 2006

A Model for the Proteolipid Ring and Bafilomycin/Concanamycin-binding Site in the Vacuolar ATPase of *Neurospora crassa*[*]

Received for publication, June 8, 2006, and in revised form, July 26, 2006 Published, JBC Papers in Press, August 15, 2006, DOI 10.1074/jbc.M605532200

Barry J. Bowman[‡1], **Mary E. McCall**[‡], **Robert Baertsch**[§], **and Emma Jean Bowman**[‡]

From the Departments of [‡]*Molecular, Cell, and Developmental Biology, and* [§]*Biomolecular Engineering, University of California, Santa Cruz, California 95064*

The vacuolar ATPase has been implicated in a variety of physiological processes in eukaryotic cells. Bafilomycin and concanamycin, highly potent and specific inhibitors of the vacuolar ATPase, have been widely used to investigate the enzyme. Derivatives have been developed as possible therapeutic drugs. We have used random mutagenesis and site-directed mutagenesis to identify 23 residues in the c subunit involved in binding these drugs. We generated a model for the structure of the ring of c subunits in *Neurospora crassa* by using data from the crystal structure of the homologous subunits of the bacterium *Enterococcus hirae* (Murata, T., Yamato, I., Kakinuma, Y., Leslie, A. G., and Walker, J. E. (2005) *Science* 308, 654–659). In the model 10 of the 11 mutation sites that confer the highest degree of resistance are closely clustered. They form a putative drug-binding pocket at the interface between helices 1 and 2 on one c subunit and helix 4 of the adjacent c subunit. The excellent fit of the *N. crassa* sequence to the *E. hirae* structure and the degree to which the structural model predicts the clustering of these residues suggest that the folding of the bacterial and eukaryotic polypeptides is very similar.

The vacuolar ATPase (V-ATPase)[2] is a component of almost all the eukaryotic cell membranes derived from the endoplasmic reticulum, *e.g.* Golgi, vacuoles, and coated vesicles (1–4). It generates an electrochemical gradient for protons, providing a driving force for metabolite transport. It also plays a major role in adjusting the pH within organelles.

In animals many diverse physiological processes depend on the function of the V-ATPase. For example, a single mutation of the enzyme in humans was shown to cause both loss of kidney function and deafness (5). The V-ATPase is critical for the growth of bone (6), and overexpression of the enzyme has been correlated with the metastasis of breast cancer cells (7). The common thread linking these physiological events is secretion of protons by specialized cells that have high amounts of V-ATPase in the plasma membrane. A high rate of proton transport by the V-ATPase appears to be a key element in the development of diseases such as osteoporosis and in the growth of certain types of tumors. These findings have led to an investigation of the use of V-ATPase inhibitors as therapeutic drugs (8, 9).

Several different classes of natural products, such as the benzolactone enamides and the chondropsins, have been shown to be potent and specific inhibitors of V-ATPases (10–12). The most widely used inhibitors are two similar macrolide antibiotics, bafilomycin and concanamycin. These molecules inhibit the V-ATPase from all eukaryotic cells that have been tested, typically with half-maximal inhibition at 0.1–5 nM when assayed *in vitro* (13–15). At higher concentrations these antibiotics also inhibit *in vivo*, and derivatives of bafilomycin were effective in treating osteoporosis in a rat model system (16).

We have been trying to identify the site on the V-ATPase at which bafilomycin and concanamycin bind and inhibit (17, 18). A precise definition of this site could be useful for development of therapeutic drugs. In addition it would lead to a much better understanding of the structure and mechanism of the V-ATPase, a large and complex enzyme. The proton-translocating part of the enzyme, named Vo, is composed of six types of subunits embedded in the membrane, with a reported stoichiometry of $a_1c_{4-5}c'_1c''_1d_1e_1$ (1, 4). ATP is hydrolyzed within the V1 part of the enzyme, a roughly globular structure connected to Vo by at least two stalks (19, 20). V1 contains eight types of subunits with a reported stoichiometry of $A_3B_3CDEFG_2H_{1-2}$. Like the F-type ATPase of mitochondria, chloroplasts, and eubacteria, the V-ATPase functions as a rotary motor. In current models, hydrolysis of ATP by the "motor" (primarily the A and B subunits) drives the rotation in the membrane of the "rotor" (composed of the D, F, c, c′, c″, and d subunits) (21–23).

In previous work we developed methods to isolate mutant strains of *Neurospora crassa* that were resistant to inhibition by bafilomycin and concanamycin (17, 18). The most strongly resistant strains, and all strains in which the V-ATPase was resistant *in vitro*, had mutations in *vma-3*, which encodes the c subunit of the enzyme. Subunit c is composed of 161 amino acids and is predicted to have four transmembrane helices. Bafilomycin and concanamycin are large enough to contact 10–20 residues within the protein. Identification of residues

* This work was supported by NCI/SAIC Contract 22XS013A from the National Institutes of Health, National Institutes of Health Grant GM058903, and a grant from the University of California Cancer Research Coordinating Committee. The costs of publication of this article were defrayed in part by the payment of page charges. This article must therefore be hereby marked "*advertisement*" in accordance with 18 U.S.C. Section 1734 solely to indicate this fact.

[1] To whom correspondence should be addressed. Tel.: 831-459-2245; E-mail: bowman@biology.ucsc.edu.

[2] The abbreviations used are: V-ATPase, vacuolar proton-translocating ATPase; F-ATPase, F-type proton-translocating ATPase; bfr, bafilomycin-resistant; bcr, bafilomycin- and concanamycin-resistant; PIPES, piperazine-*N*,*N*′-bis(2-ethanesulfonic acid).

involved in binding would allow us to test various models for the structure of the c subunit and for the arrangement of c subunits within the rotor sector.

Several models for the c subunits (c, c′, and c″) of the V-ATPase have been proposed. The sequence of each half of the c subunit of the V-ATPase is ~22% identical to the sequence of subunit c in F-type ATPases, which contain only two transmembrane helices (24). High resolution structures derived from NMR and x-ray crystallography data are available for the c subunit of F-ATPase (25–27). In our previous model for the bafilomycin-binding site, we assumed the V-ATPase c subunit had a similar structure. Forgac and co-workers (28), using site-directed mutagenesis and cross-linking studies, proposed a model for part of subunit c′, which has a high degree (53% in *Saccharomyces cerevisiae*) of sequence identity to subunit c. Harrison and co-workers (29–31) proposed a significantly different model for subunit c, based on cysteine replacement mutagenesis and analysis of lipid-accessible sites. A major advance was made in the last year with the report of the crystal structure of part of the rotor of the V-type Na^+-ATPase from *Enterococcus hirae* (32). The rotor contains 10 copies (40 transmembrane helices) of the NtpK subunit, which appears to be the homolog of subunit c in eukaryotic V-ATPases.

We earlier proposed a model in which the bafilomycin-binding site was at the interface between helix 4 of one c subunit and helices 1 and 2 of an adjacent c subunit (18). In this study we describe experiments to select additional bafilomycin- and concanamycin-resistant strains of *N. crassa* and to generate site-directed mutants to further test models of the drug-binding site. Eleven residues in subunit c, when mutated, change the affinity for bafilomycin by at least 4-fold. To construct a better model we fit the *N. crassa* amino acid sequence to the structure of the rotor from *E. hirae* and analyzed the positions of residues altered in the drug-resistant mutants.

EXPERIMENTAL PROCEDURES

Random Mutagenesis and Analysis of Mutant Strains—The procedures for growth of *N. crassa*, UV mutagenesis, isolation of vacuolar membranes, and V-ATPase assays were as described previously (17, 18, 33, 34). Selective media for drug-resistant strains contained Vogel's minimal medium (35) supplemented with 2% sucrose and nutritional supplements as needed, adjusted to pH 7.2, and containing either 1.0 μM bafilomycin A1 or concanamycin C for selection of bfr (bafilomycin-resistant) and bcr (bafilomycin- and concanamycin-resistant) strains, respectively. For all strains resistance to bafilomycin and concanamycin was measured in duplicate titrations for at least two independent preparations of vacuolar membranes. The average of a least two assays is given in Tables 1 and 2.

Site-directed Mutagenesis of vma-3—*N. crassa* strains lacking the V-ATPase grow very slowly and do not produce conidia, the asexual spores typically used for transformation (36). Therefore, a heterokaryon was constructed in which one type of nucleus lacked the *vma-3* gene, whereas the other type of nucleus was *vma-3*$^+$, allowing nearly normal growth and conidiation (Fig. 1). Robert Metzenberg (California State University, Northridge, CA) provided both guidance and the required strains and plasmids. Strain RLM 79-28 is *mat-a*,

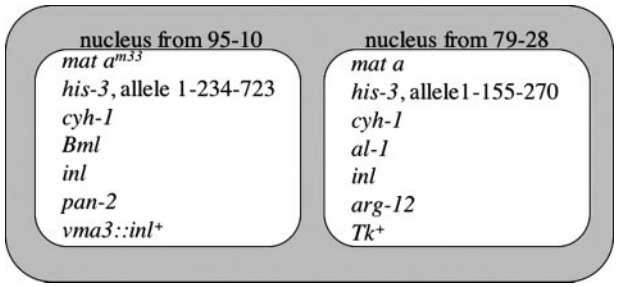

FIGURE 1. **Genotype of the heterokaryon strain TF18.**

cyh-1 (cycloheximide-resistant), *al-1* (albino), *inl* (requires inositol), *arg-12* (requires arginine), and *his-3*, allele 1-155-270 (requires histidine and cannot be complemented by the plasmid pBM61). We transformed this strain with the plasmid pHygTk, which confers resistance to hygromycin and also contains *Tk*$^+$, the gene for thymidine kinase (37). The *Tk*$^+$ gene confers dominant sensitivity to 5-fluorouridine-2′deoxyriboside. Strain RLM 95-10 is *mat-a*^{m33} (an allele of mating type a that is both heterokaryon-compatible and sexually competent), *cyh-1*, *Bml* (encodes β-tubulin and confers resistance to benomyl), *inl*, *pan-2* (requires pantothenate) and *his-3*, allele 1-234-723 (can be complemented by pBM61). Co-inoculation of the two strains on medium containing histidine (150 μg/ml) and inositol (100 μg/ml), but lacking pantothenate and arginine, generated the heterokaryon. To delete the *vma-3* gene, we used the plasmid pVMA3/inl, which contains a functional copy of the *inl* gene flanked on each side by 2 kb of upstream and downstream regions of the *vma-3* gene (38). Conidia from the heterokaryon were transformed with this plasmid by electroporation; 40 *inl*$^+$ colonies were selected. It was necessary to modify the transformation procedure, using α-D-methyl-glucoside as osmoticum because sorbitol contains small amounts of inositol. Conidial isolates from the colony named TF18 grew slowly with the morphology observed in vma-null strains (36) when grown on medium that contained histidine, pantothenate, 1 mM uracil, and 1 μM 5-fluorouridine-2′deoxyriboside. These homokaryotic pan$^-$ strains, named Δvma3-TF18, had no detectable *vma-3* coding region by Southern blot analysis (data not shown). Transformation of TF18 with a functional *vma-3* gene, described below, yielded homokaryotic pan$^-$ isolates with a nearly normal growth phenotype.

To generate mutations in the *vma-3* gene, we constructed a plasmid that contained *vma-3* with 750 bp upstream and 1040 bp downstream of the open reading frame. By using the primers CCGGATCCAGGCAGCAGATTCGTTTTG and GCGGATCCACCTACCTACGATGTACC, we amplified a 2.8-kb fragment and inserted it into the plasmid pCR2.2-TOPO (Invitrogen). This plasmid was then digested with NotI + SpeI, and the 2.8-kb fragment was inserted into NotI/SpeI-digested pBM61, a plasmid developed for targeted integration at the *his-3* locus of *N. crassa* (39). The resulting plasmid was named pMM1. Mutations were generated in pMM1 by the QuikChange kit (Stratagene) and verified by sequencing the *vma-3* open reading frame. The TF18 strain was transformed by electroporation, and histidine prototrophs were selected. Conidia from these isolates were streaked on plates containing Vogel's salts, 2% sorbose, 0.05% glucose, 0.05% fructose, plus or minus pantothe-

nate (10 μg/ml). DNA was prepared from the pan⁻ strains using the DNeasy plant kit (Qiagen). The protein coding region of *vma-3* was amplified and sequenced at the DNA Sequencing Facility, University of California, Berkeley. Procedures for isolation of vacuolar membranes and assays for the effect of inhibitors on V-ATPase activity were the same as for strains produced by random mutagenesis.

Generation of Mutations in Subunit a—Vph-1-RIP, a null strain for subunit a, has been described previously (38). The plasmid pFO1 contains a 3.9-kb fragment with the wild type *vph-1* gene inserted into the pBM61 vector. Mutations were generated in this plasmid with the QuikChange procedure. The mutated plasmids were introduced into the *his-3 mat-A* strain by electroporation, and histidine prototrophs were selected. These were crossed with a heterokaryon composed of *vph-1*^{RIP} *arg-12 mat-a* and *ad-3B cyh-1 mat-a*^{m1} (FGSC 4564). (The latter nucleus is functionally sterile in the cross but serves as a "helper" allowing conidiation.) To obtain progeny with a mutated *vph-1* gene at the *his-3* locus and the *vph-1*^{RIP} allele at the endogenous *vph-1* locus, we screened for *mat-A* (linked to *his-3*) and *arg-12* (linked to *vph-1*). The genotype of strains was confirmed by using PCR to selectively amplify the ectopic and endogenous *vph-1* genes, which were then sequenced. Double mutants, altered in both *vph-1* and *vma-3,* were obtained by crossing. For example, bfr-217 (A121T in *vma-3*) was crossed with vph-1-L743T, *vph-1*^{RIP}, *arg-12*, *mat-A*. Spores were germinated on medium adjusted to pH 7.2 containing 1 μM bafilomycin. After identification of drug-resistant isolates that were *mat-A*, *arg-12*, the ectopic and endogenous *vph*-1 genes and the *vma-3* gene were amplified by PCR and sequenced.

Building a Molecular Model—Starting with the solved structure of the membrane rotor of the V-ATPase from *E. hirae* (Protein Data Bank code 2BL2), we fit the *N. crassa* protein sequence to this model using the MacLachlan algorithm (40) as implemented in the program ProFit. Because the *N. crassa* protein has an extra histidine at position 82 and has different ends, we used the Rosetta loop modeler to rebuild the structure from residues 1–3, 80–84, and 153–161, while holding the remainder of the structure fixed (41). As a final step, we fit 10 copies of the model in the shape of a cylinder and ran the full Rosetta model without constraints in "relax mode" in order to evaluate the stability of the structure using parameters-relax-minimize-farlx. The Rasmol program (42) was used to generate molecular graphics.

Materials—The bafilomycin A1 used in these experiments was a gift from Dr. C. Farina and Dr. S. Gagliardi (NiKem Research, Milan, Italy). Concanamycin C was a gift from Dr. A. Zeeck (University of Göttingen) and Dr. K. Altendorf (University of Osnabrück).

RESULTS

Isolation of Drug-resistant Strains by UV Mutagenesis—As described in previous reports, strains of *N. crassa* resistant to bafilomycin can be generated by UV irradiation of conidia (vegetative spores) (17, 18). By using this method we obtained two strains with mutations in the *vma-3* gene at sites not identified previously. We prepared vacuolar membranes from these strains and compared the K_i values for bafilomycin and concanamycin inhibition of V-ATPase activity to the K_i values for the wild type strain 74A. The data (Table 1) were obtained by measuring the concentration of each drug that inhibited ATPase activity by 50%, as in the experiment shown in Fig. 2. The A121T mutation (strain bfr217) had specific V-ATPase activity comparable with the wild type, was weakly resistant to bafilomycin (2 times), and had little resistance to concanamycin. The G61S mutation (bfr200) was the most strongly resistant single mutant strain we have obtained. The V-ATPase-specific activity was approximately half that of wild type, but the K_i value for bafilomycin was 90-fold greater, and the K_i value for concanamycin was 5-fold greater than for the wild type enzyme.

TABLE 1
V-ATPase activity and sensitivity to bafilomycin (Baf) and concanamycin (CCC) in strains obtained by random mutagenesis

Mutation in subunit c	V-ATPase activity	-Fold increase in resistance to Baf	-Fold increase in resistance to CCC
	μmol/min/mg		
Single mutations, bfr strains			
Wild type(74A)	4.7	1.0	1.0
T32I[a]	2.1	68.0	3.1
I39F	1.6	26.0	2.5
G61S	1.9	90.0	5.0
A121T	4.1	1.9	1.7
F136L[a]	2.4	13.0	1.0
L140F[a]	3.3	3.7	1.6
Y143H[a]	2.8	17.0	2.6
Y143N[a]	3.4	20.0	2.9
Double mutations, bcr strains			
T32I + I54F[a]	2.2	325.0	39.0
T32I + V55A[a]	3.8	37.0	5.6
T32I + M130I[a]	2.7	215.0	5.6
T32I + L132F[a]	1.5	286.0	9.9
I39F + G38S	1.6	86.0	8.5
I39F + I54F	2.2	117.0	12.0
A121T + I39F	2.6	103.0	10.0
A121T + I54F	3.8	27.0	11.0
A121T + G61A	1.9	350.0	97.0
A121T + G61C	0.8	450.0	84.0
A121T + Y143H	2.4	51.0	13.0
A121T + Y143N	1.9	35.0	13.0

[a] Data were published previously (17, 18).

As in previous mutagenesis experiments, hundreds of colonies appeared on the selective medium; however, most grew slowly on medium containing bafilomycin. Mutations in the *vma-3* gene were found only in isolates that grew vigorously and with relatively normal hyphal morphology. We reasoned that some of the weakly growing strains could be mutated in other V-ATPase subunits or had mutations that impaired the function of the V-ATPase. We prepared vacuolar membranes from 21 strains that were more weakly resistant as assessed by growth on bafilomycin. None of these yielded V-ATPase showing significant resistance to bafilomycin *in vitro* (data not shown).

To identify additional residues involved in drug binding, we subjected several of the bfr strains to further mutagenesis. None of the bfr strains grow well on alkaline medium (pH 7.2) containing 1 μM concanamycin. We had observed previously that a second mutation could confer significant resistance to concanamycin and increase the resistance to bafilomycin. Mutagenesis of the bfr34 strain produced two double mutant strains, the original I39F plus G38S or I54F (Table 1) mutations in *vma-3*. Using the bfr 217 strain (A121T) we isolated six dif-

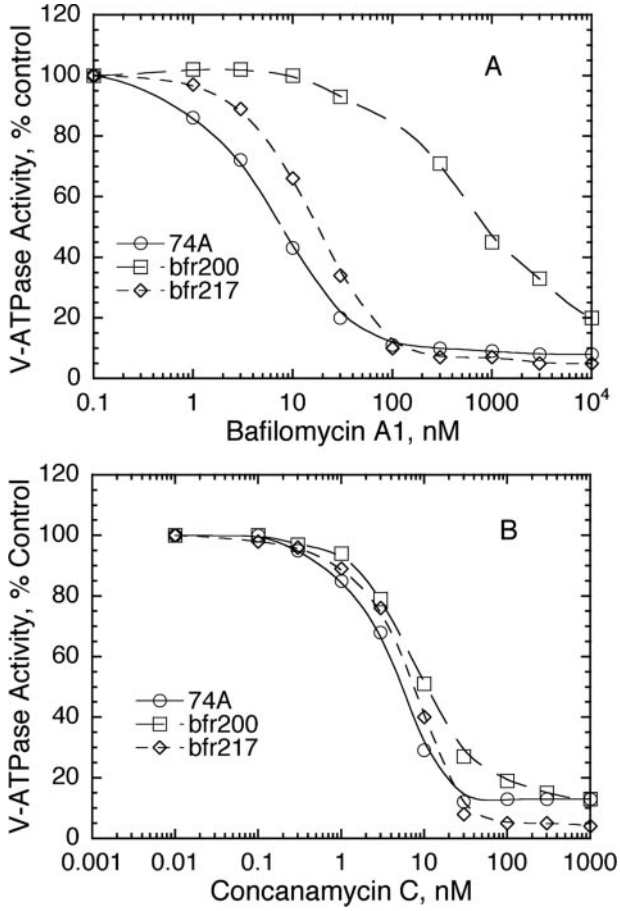

FIGURE 2. **The effect of inhibitors on V-ATPase activity in wild type and mutant strains.** ATP hydrolysis was measured in purified vacuolar membranes (18). The assay mixture contained 5 mM Na_2ATP, 5 mM $MgSO_4$, 10 mM NH_4Cl, 10 mM PIPES, adjusted to pH 7.5 with Tris base. Inhibitors were added from 10 mM stock solutions in dimethyl sulfoxide. The reaction was started by the addition of 2 μg of membrane protein per 0.5-ml assay mixture and was stopped after 25 min at 37 °C. *74A* is the wild type strain; *bfr200* has the mutation G61S; and *bfr217* has the mutation A121T.

ferent types of double mutants, each with the original A121T mutation plus a second mutation in *vma-3* (Table 1). No new mutant strains were obtained by mutagenesis of bfr 21 (F136L). In most cases the new double mutants had significantly increased resistance to both bafilomycin and concanamycin compared with the original single mutant strain. Mutation at A121T plus G61A or G61S produced V-ATPase that was ~400-fold more resistant to bafilomycin and ~100-fold more resistant to concanamycin when compared with enzyme from the wild type strain. The specific activity of the V-ATPase in the A121T/G61A double mutant strain was ~40% that of the wild type (Table 1), indicating that these mutations did not grossly alter the structure of the V-ATPase. In these mutagenesis experiments, all but one (G38S) of the changed residues had been identified previously, either in single mutant strains or as second mutations in combination with T32I. Although the mutagenesis experiments reported in this paper produced a total of 29 *vma-3* mutant strains, only three were in residues not identified previously. These results suggest there are not a large number of additional residues involved in binding the drugs. Alternatively, mutations of other important residues may significantly inactivate the enzyme. Fig. 3 shows the positions of all residues changed by random mutagenesis.

Test of Bafilomycin and Concanamycin Resistance in Site-directed Mutants—Five of the sites identified by UV mutagenesis (Gly-38, Ile-54, Val-55, Met-130, and Leu-132) were found only in strains with double mutations. To assess the drug resistance of V-ATPase with single mutations at these sites, we used site-directed mutagenesis. As described under "Experimental Procedures," we generated a strain, Δvma3-TF18, in which the entire protein-coding region of the *vma-3* gene was replaced by the *inl* gene. The phenotype of this strain was the same as that of the vma-1-RIP mutant strains of *N. crassa* reported previously (36). The strain grew slowly at pH 5.8, failed to grow in medium above pH 7, and had severe morphological defects. Plasmids containing the *vma-3* gene were targeted to the *his-3* locus in the TF18 strain, and homokaryotic pan$^-$ strains were isolated. Insertion of the wild type *vma-3* gene restored normal morphology and nearly normal growth rates. Vacuolar membranes from the rescued strain, named MM1, had comparable specific activity for ATP hydrolysis and had the same K_i value for bafilomycin and concanamycin as V-ATPase from the wild type strain (Table 2). As a further control we used site-directed mutagenesis to construct strains with the F136L (bfr21) and T32I (bfr33) mutations in *vma-3*. V-ATPase from these strains was resistant to bafilomycin with K_i values comparable with those measured in the corresponding strains obtained by UV mutagenesis (Table 2).

We constructed strains with the mutations G38S, I54F, V55A, M130I, and L132F. The strains grew at pH 7.2, had normal morphology, and produced conidia, indicating that the V-ATPase was functional. The V-ATPase activity in vacuolar membranes was ~50% of the wild type level, except for the L132F strain, which was 20%. Three strains, G38S, V55A and M130I, showed 2–3-fold increases in the K_i for bafilomycin and concanamycin. The I54F strain was most resistant, 12 times wild type for bafilomycin. The L132F strain had the highest level of resistance to concanamycin of any single-mutant strain, 7.5 times, and was unusual in showing equal resistance to both bafilomycin and concanamycin.

We previously proposed a model for the structure of subunit c and the bafilomycin/concanamycin-binding site (18). To test this model we selected three residues in each of the four membrane helices. The rationale was to select residues on different faces of each helix (~120° apart) positioned in the cytosolic half of the polypeptide, the half that was implicated in drug binding. Table 2 shows the mutated sites and the phenotypes of these strains. In contrast to the results with the UV-induced mutants, the V-ATPase activity was less than 20% of the wild type level in half of the site-directed mutant strains. These strains showed only a modest increase in the K_i values for bafilomycin and concanamycin. The most resistant were I50F, V57A, and I131F with 4.4- to 5.2-fold increases in the K_i values for bafilomycin.

Analysis of Strains with Mutations in Subunit a—In the F-ATPase of *S. cerevisiae*, mutations in both the a and c subunits confer resistance to the antibiotic oligomycin (43). Fig. 4 shows an alignment of a region of the a subunits from *S. cerevisiae* F-ATPase (Atp6p), *S. cerevisiae* V-ATPase (Vph1p), and *N. crassa* V-ATPase (Vph-1p). Mutations of the two marked resi-

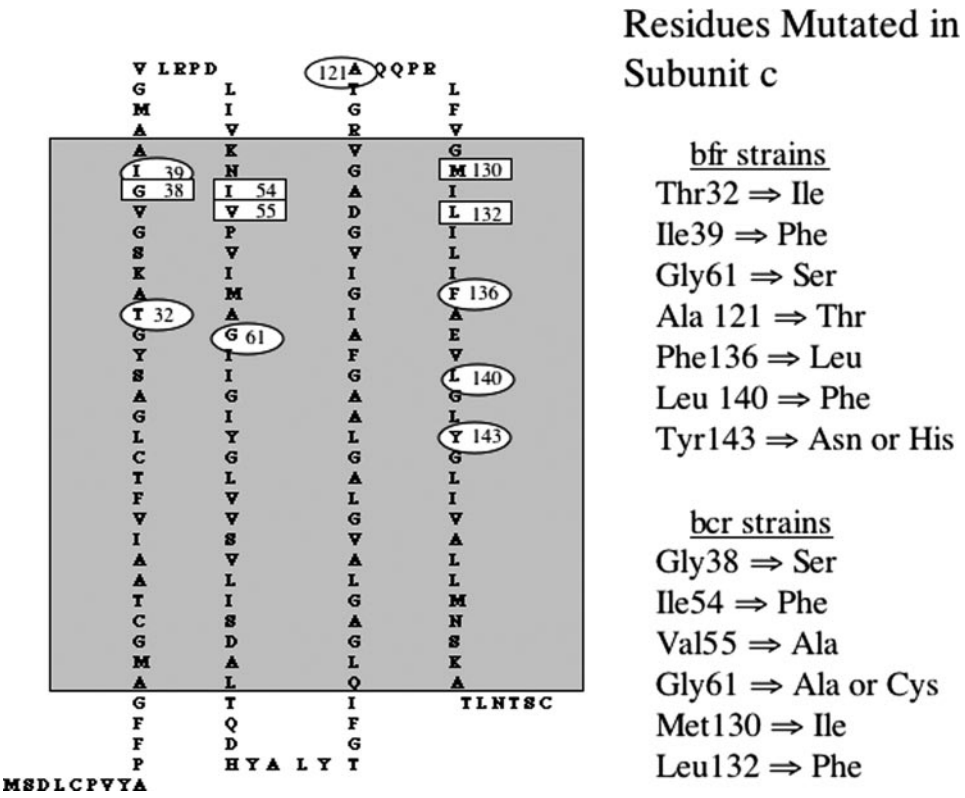

FIGURE 3. **Secondary structure of subunit c showing positions of mutations that confer resistance to bafilomycin.** Subunit c is modeled with four transmembrane helices. The *boxed region* shows the approximate position of the lipid bilayer. The relative depth of each residue within the bilayer is based on the model derived from the structure of *ntpK* in *E. hirae* as discussed in the text. Only residues identified by random mutagenesis are shown, either in *rectangles* (bcr strains) or *ovals* (bfr strains).

dues in F-ATPase subunit a conferred resistance to oligomycin. The V-type and F-type a subunits share little sequence identity. However, this region contains a critical arginine residue shown to have a central role in proton translocation in both types of ATPase (44). We constructed two strains of *N. crassa* with site-directed mutations at the positions shown in Fig. 4. In the I739M strain the K_i value for bafilomycin was essentially the same as in the wild type (1.1-fold higher). In the L743T strain the K_i value for bafilomycin was 1.8-fold that of wild type. Wang *et al.* (47) reported the same results for *S. cerevisiae*; I720M was the same as wild type, and L724A was 1.8-fold more resistant.

Because of the strong increase in resistance to bafilomycin caused by second mutations in subunit c, we wanted to see if a mutation in subunit c might enhance the resistance of the two subunit a mutants. We made genetic crosses between bfr strains and the two *vph-1* site-directed mutant strains to generate strains with mutations in both the c and a subunits as follows: A121T (c) + L743T (a), I39F (c) + I739M (a), I39F (c) + L743T (a), F136L (c) + I739M (a), and F136L (c) + L743T (a). In all of these strains the K_i value for bafilomycin was not significantly different from the K_i value for the strain with the single mutation in subunit c (data not shown).

Using the Structure of the Proteolipid Ring of E. hirae to Model the c Subunit of N. crassa—The most detailed structural data available for the c subunit of a V-ATPase was obtained recently for the bacterium *E. hirae* (32). The *Ntp* genes in this organism encode a V-type ATPase that pumps sodium. Crystals were obtained for a ring of 10 proteolipid subunits (encoded by *NtpK*), and the structure was determined at a resolution of 2.1 Å. Although a large degree of evolutionary divergence has occurred between *E. hirae* and *N. crassa*, the respective K and c subunits from these organisms are similar. The sequences can be aligned with a gap of only one amino acid between the second and third helices; 24% of the residues are identical (Fig. 5). By comparison, an alignment of the c subunits from the V-ATPase of *N. crassa* and the F-ATPase of another fungus, *S. cerevisiae*, have only 17% sequence identity.

We constructed a model of the *N. crassa* subunit c, using the coordinates for the NtpK protein (Fig. 6*A*). In this version of the model we did not attempt to change the stoichiometry of subunits or to generate different models for the c′ and c″ subunits. The *N. crassa* sequence fit to the *E. hirae* structure remarkably well. Relaxation of the constraints in the initial model caused no significant change in the structure.

If the model is a good representation of the *N. crassa* c subunit, and if the residues altered in the bafilomycin-resistant mutants form part of the drug-binding site, then we predict that most of these residues should be clustered around a space approximately the size of the drugs. In Fig. 6*B*, the ring of c subunits is viewed from the side, highlighting the 11 residues that confer the most resistance when mutated. The structures of bafilomycin and concanamycin are also shown to scale. The model predicts that the bafilomycin-binding site is in the cytosolic half of the c-ring spanning a space approximately equivalent to the size of the drugs.

The model predicts the relative orientation of each amino acid side chain, *e.g.* its depth in the membrane and whether it faces a neighboring subunit or another helix within a subunit. This model, used to construct Figs. 3 and 6–8, predicts a tighter clustering of the residues mutated in the drug-resistant mutant strains when compared with the previous model based on the crystal structure of the c subunit of the *S. cerevisiae* F-ATPase (18). The *E. hirae* data show the positions of lipids and predict that fewer residues will protrude above the lipid bilayer on the cytosolic side of the membrane. In addition, the positions of all residues in helices 1–3 are moved toward the luminal side of the membrane relative to residues in helix 4. For example, in the previous model Ile-39 was above the surface of the bilayer, but the new model places it in the same depth in the bilayer as Met-130.

Fig. 6*C* shows the positions of four transmembrane helices that form the interface between two c subunits. The positions of amino acids in the cytosolic half of the four helices are pre-

TABLE 2

V-ATPase activity and sensitivity to bafilomycin (Baf) and concanamycin (CCC) in strains obtained by site-directed mutagenesis

Mutation in subunit c	V-ATPase activity	-Fold increase in resistance to Baf	-Fold increase in resistance to CCC
	μmol/min/mg		
Controls			
Wild type(74A)	4.7	1.0	1.0
MM1, SD wild type	4.3	1.0	1.0
T32I (bfr33)	2.1	68.0	3.1
T32I SD mutant	1.8	80.0	4.4
F136L (bfr21)	1.7	13.0	1.0
F136L SD mutant	1.2	17.0	1.0
Site-directed mutants from bcr strains			
G38S	2.5	2.0	2.5
I54F	2.1	12.0	3.9
V55A	2.9	3.2	2.5
M130I	2.3	2.7	1.3
L132F	0.8	7.8	7.5
Helix 1 site-directed mutants			
C25A	0.9	2.4	2.1
A28T	0.2	0.5	0.3
A33T	4.9	1.6	1.5
Helix 2 site-directed mutants			
L49F	0.7	2.2	0.7
I50F	3.2	4.4	1.9
V57A	4.0	5.2	2.0
Helix 3 site-directed mutants			
A101T	2.5	1.7	1.4
G106S	1.9	1.9	0.8
F107L	4.5	3.1	2.1
Helix 4 site-directed mutants			
G129A	5.2	3.6	1.6
I131F	0.7	4.8	1.7
K154E	0.9	1.4	1.0

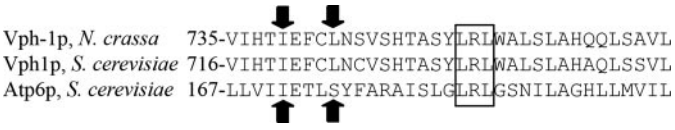

FIGURE 4. **Mutation sites in subunit a.** Mutations in the *ATP6* gene of the *S. cerevisiae* F-ATPase, marked by *arrows*, confer resistance to oligomycin. The corresponding regions of subunit a from *N. crassa* and *S. cerevisiae* V-ATPases are aligned with reference to the Arg residue implicated in proton transport (in *box*). The two residues in *N. crassa* changed by site-direct mutagenesis are also marked by *arrows*.

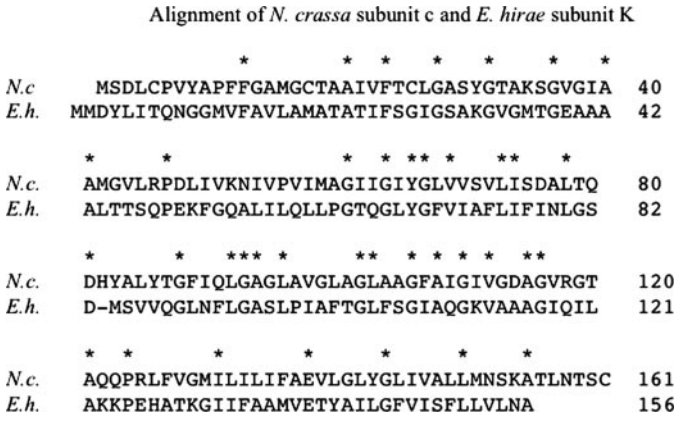

FIGURE 5. **Aligned protein sequences of *E. hirae* (*E.h.*) ntpK protein and *N. crassa* (*N.c.*) subunit c.** Identical residues are marked with an *asterisk*.

sented as helical wheel diagrams in Fig. 7. The increase in the K_i value for bafilomycin is shown for each of the 22 mutated positions. The most striking observation is that 10 of the 11 mutations that conferred the most resistance (4-fold or greater) lie in a pocket formed by helices 1, 2, and 4. Helix 3 is furthest away from this pocket, consistent with the result that we obtained no helix 3 mutants by random mutagenesis. The three mutations in helix 3 generated by site-directed mutagenesis were weakly resistant (1.7–3.1 times). Six of seven other mutations at sites

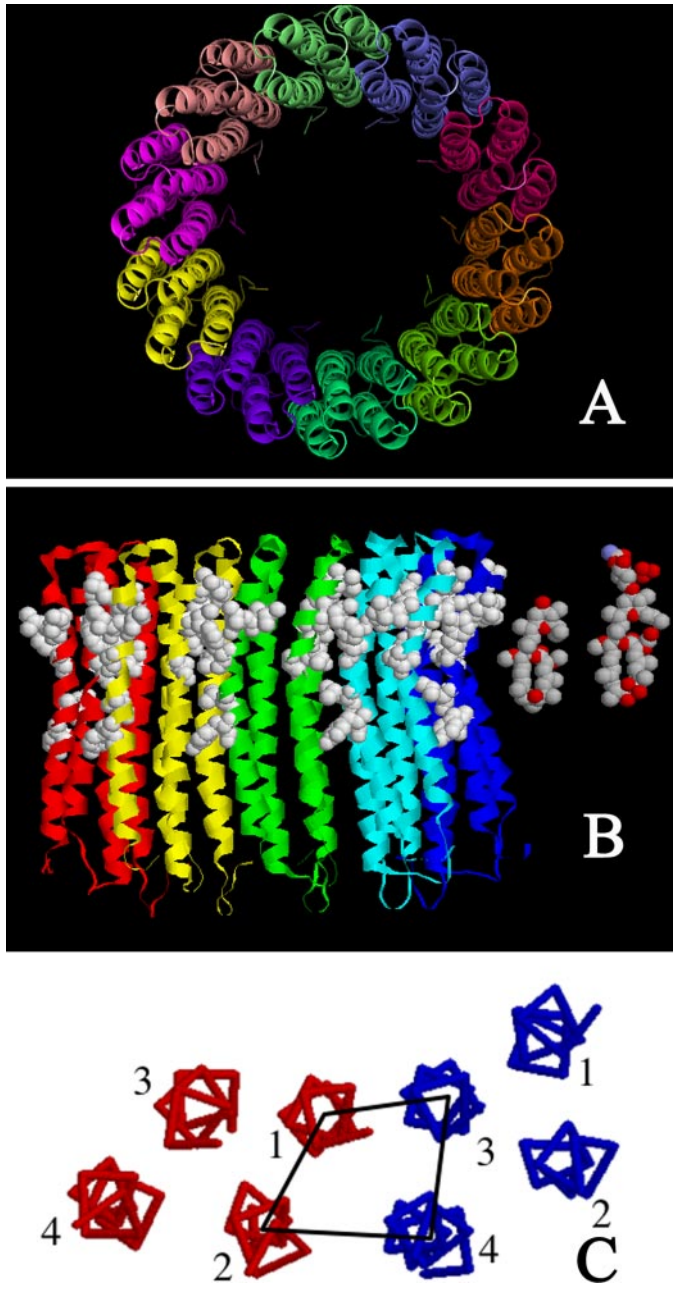

FIGURE 6. **Model of the structure of a ring of 10 c subunits from *N. crassa*.** *A*, view of the structure from the cytosolic side of the membrane. The model is based on the structure of the *E. hirae* ntpK protein as described in the text. Individual subunits are in different colors. *B*, view of the structure from within the plane of the membrane. *White* space-filling models of the 11 residues that confer the highest degree of drug resistance are shown, along with space-fill models of bafilomycin (*center*) (46) and concanamycin (*right*) (58). *C*, positions of helices that form the interface between c subunits. The region of the protein containing residues implicated in binding bafilomycin is viewed from above. The backbones of two polypeptides are shown, using residues 27–40 in *helix 1*, 52–64 in *helix 2*, 104–117 in *helix 3*, and 129–144 in *helix 4*. The *lines* mark the spacing between the centers of the helices.

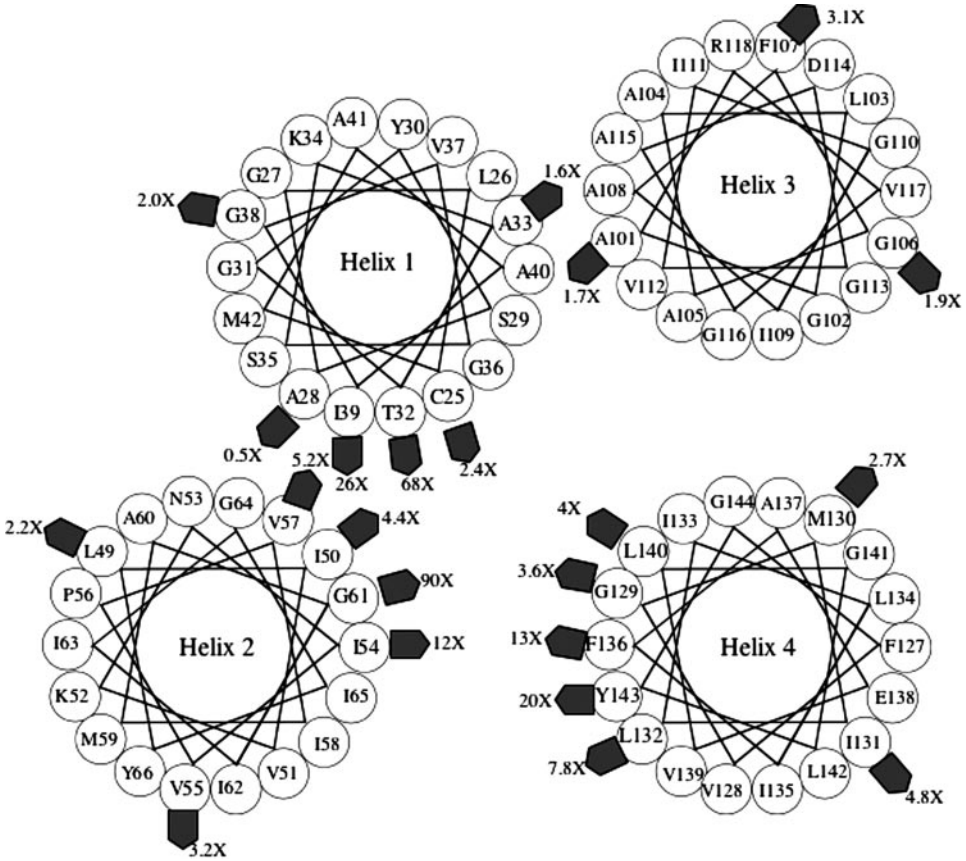

FIGURE 7. **Positions of mutated residues on a helical wheel diagram.** The spacing of the helical wheels, based on the model in Fig. 6, represents the interface between two subunits. *Arrows* mark the positions of residues mutated by random mutagenesis and site-directed mutagenesis. The *number* by each *arrow* is the change in the K_i value for bafilomycin.

not in this pocket also conferred only weak drug resistance (0.5–3.2 times). The exception, I131F, was only slightly more resistant (4.8-fold).

To obtain a three-dimensional view of the predicted binding pocket, we constructed a model with parts of two neighboring c subunits, colored *red* and *blue* in Fig. 8*A*. Each subunit contained Gly-27 to Ala-40 in helix 1, Lys-52 to Gly-64 in helix 2, Ala-104 to Val-117 in helix 3, and Gly-129 to Gly-144 in helix 4. The model predicts that essentially all of the side chains of residues conferring strong resistance are on the outer surface of each subunit. Mutated residues on helices 1 and 2 (Fig. 8*A*, *white* and *yellow*) face mutated residues on helix 4 (*green*) in the neighboring subunit. All of these residues face away from helix 3 and the interior of each subunit. The simplest interpretation of these data is that bafilomycin and concanamycin intercalate between c subunits in this binding pocket. A space-filling model of the c-ring with the positions of mutated residues highlighted is shown in Fig. 8*B*.

DISCUSSION

The objectives of these experiments have been to define, in as much detail as possible, the binding site of bafilomycin and concanamycin. In doing so we also hoped to generate a good model for the structure of c subunits of the V-ATPase, which play a key role in the function of the enzyme. In previous reports we used structural data for the c subunit of F-ATPases to model the bafilomycin-binding site. Analysis of mutations in drug-resistant strains indicated that helices 1, 2, and 4 were involved, but a more precise definition of the binding site was not possible (18).

The publication of the structure of the K-ring from *E. hirae* V-ATPase offered the opportunity to build a much better model (32). Although the *E. hirae* K subunit and eukaryotic c subunits have diverged significantly in sequence, the polypeptides are nearly identical in length and form a relatively simple 4-helix structure. We constructed a model by "threading" the *N. crassa* sequence onto the *E. hirae* structure and then used the Rosetta program to allow reorientation of the structure as driven by the *N. crassa* amino acid sequence. Remarkably, the "relaxed" structure changed very little, strongly suggesting that the K and c polypeptides fold into very similar structures.

We used a genetic approach to identify residues involved in drug binding. By random mutagenesis we have isolated 55 independent bafilomycin-/concanamycin-resistant strains that have amino acid changes at 12 different sites, all in the c subunit of the V-ATPase. Site-directed mutagenesis targeted another 12 residues. Ten of the 11 mutations that conferred the strongest resistance to bafilomycin (4–90 times) are predicted to be remarkably close to each other in the molecular model. Most of the residues lie on opposing faces of the outer helices 2 and 4. The two mutation sites on the inner helix 1 point into the space between helices 1 and 2. Bafilomycin is a relatively flat molecule, ~15 Å long and the width of an α-helix (46). Thus, all 10 of the residues predicted to be in the binding pocket could make molecular contacts with the drug. The model also offers an explanation for the absence of mutations in helix 3; it is not positioned near the predicted drug-binding site. Overall, the excellent agreement between the predicted positions of residues in the structural model and the degree to which mutation of those residues affected inhibition by bafilomycin strongly support the validity of the model for eukaryotic V-ATPases.

Mutation of residues not in the putative binding pocket, including those in helix 3, typically produced a 2–3-fold increase in the K_i for bafilomycin. This suggests that a small distortion in the structure of subunit c is likely to change the binding affinity for the drugs. One of the mutations we generated in subunit a, and also three within the more extensive set of subunit a mutations analyzed by Wang *et al.* (47), conferred the same degree of resistance, ~2-fold. Using a

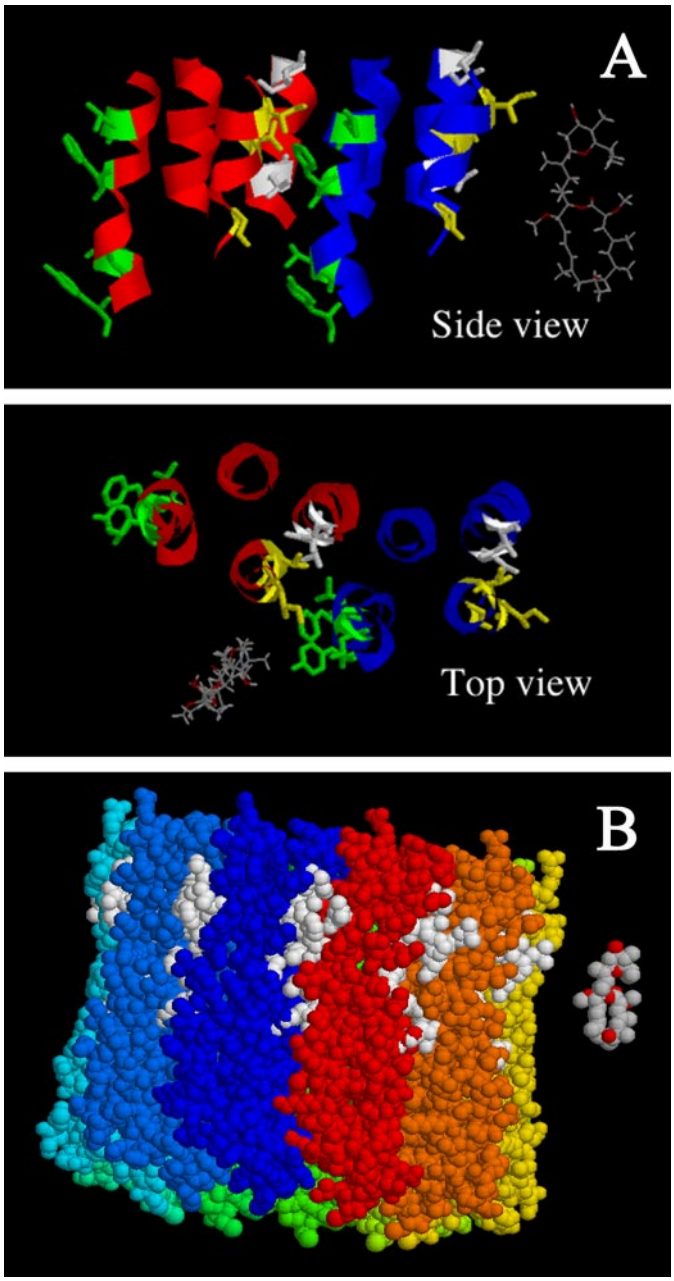

FIGURE 8. *A, side view* and *top view* of a model of the bafilomycin-binding site. Two adjacent c subunits, in *red* and *blue*, and bafilomycin are shown. The side chains of 10 residues implicated in drug-binding are in *white* (helix 1), *yellow* (helix 2), and *green* (helix 4). *B,* a space-fill model of the ring of 10 c subunits, each a different color, is shown with 10 residues in the putative drug-binding pocket in *white*. Bafilomycin on the *right* is shown to the same scale.

fluorescence quenching assay, Whyteside *et al.* (48) reported that concanamycin bound equally well to isolated preparations of either Vo or proteolipid subunits, suggesting that subunit a was not required for binding. Our results suggest that the mutated residues in subunit a may not form part of the drug binding pocket. Indeed the residues that confer resistance are predicted to lie above the membrane bilayer. However, the results are consistent with the idea that drug binding occurs when c subunits are in contact with subunit a because changes in subunit a can affect the affinity of binding.

In using the *E. hirae* data to model the ring of c subunits of *N. crassa,* we did not deal with two important differences, stoichiometry and subunit c diversity in eukaryotes. The best biochemical data, obtained with the bovine V-ATPase, indicated that the V-ATPase had six proteolipid subunits (49). A subsequent analysis of the *E. hirae* enzyme, using electron microscopy, suggested seven proteolipid subunits (50). The earliest biochemical analyses of F-ATPases predicted six proteolipids per ring (51, 52). By measuring the ^{35}S content of subunits in the *E. coli* F-ATPase, a stoichiometry of 10 ± 1 was predicted (53), in good agreement with subsequent crystal structures that revealed 10 and 11 proteolipid subunits (25, 27). The *N. crassa* amino acid sequence fits surprisingly well to the model derived from x-ray crystallography, with 10 proteolipid subunits. V-ATPases have an additional subunit, named d in eukaryotes and C in *E. hirae* and *Thermus thermophilus,* which appears to sit on top of, and project into, the center of the proteolipid ring. A crystal structure has been reported for subunit C of *T. thermophilus* (54). Murata *et al.* (32) argue that the C subunit can be fit well into the *E. hirae* structure, supporting the validity of the 10 subunit model. Subunit d from *N. crassa* has a similar size and sequence to the bacterial protein (55). The reasons for the discrepancies between some of the biochemical/electron microscopy determinations and the crystallographic structures in predicting proteolipid stoichiometry remain unresolved.

In addition to subunit c, the proteolipid ring of *N. crassa* and other fungi includes at least one copy each of c′ and c″ for each subunit (38, 56), which we did not attempt to model in this report. Subunit c″ has an extra N-terminal helix. Otherwise, the sizes and sequences of subunits c, c′, and c″ are similar and likely to fold into similar structures. Of the 11 residues postulated to be in the binding pocket in the subunit c model, 10 are identical in subunit c′; only 2 are identical in subunit c″. The interface between c and c′ could be a drug-binding site. Mutating only subunit c′ in *S. cerevisiae* was not sufficient to confer resistance to the drugs (18); however, the c′ mutant strains retained high affinity binding sites between c subunits. To evaluate binding to subunit c′ more definitively, we will need to examine strains with mutations in both c and c′ subunits.

Do bafilomycin and concanamycin bind at the same site on the V-ATPase? Although the two macrolide compounds have similar structures, they are not identical. Concanamycin, a larger molecule, might have more contact points and bind more tightly. A derivative of concanamycin has been shown to bind to subunit c in *Manduca sexta,* although the specific site was not identified (57). Single and double mutations typically cause a much larger increase in the K_i value for bafilomycin than for concanamycin (Tables 1 and 2). Nevertheless, the six mutations that cause the largest changes in K_i values for concanamycin all lie within the binding pocket we hypothesize for bafilomycin. The effects of individual mutations are hard to explain. F136L increases the K_i value for bafilomycin 13-fold but has essentially no effect (1.2-fold) on resistance to concanamycin. On the other hand, changing a neighboring residue, L132F, generates a strain that is 8-fold resistant to both drugs. Heterogeneity of binding sites might help to explain why the mutations we analyzed had different effects on binding of bafilomycin *versus* concanamycin. By examining strains with multiple mutations in

subunits c, c′, and c″, we may be able to determine whether the two drugs bind differently at the interface between different proteolipid subunits.

Acknowledgments—We thank Carol Rohl and Craig Lowe for helpful discussions in using Rosetta for building models for this study.

REFERENCES

1. Nishi, T., and Forgac, M. (2002) *Nat. Rev. Mol. Cell Biol.* **3,** 94–103
2. Sun-Wada, G. H., Wada, Y., and Futai, M. (2004) *Biochim. Biophys. Acta* **1658,** 106–114
3. Beyenbach, K. W., and Wieczorek, H. (2006) *J. Exp. Biol.* **209,** 577–589
4. Kane, P. M. (2006) *Microbiol. Mol. Biol. Rev.* **70,** 177–191
5. Karet, F. E., Finberg, K. E., Nelson, R. D., Nayir, A., Mocan, H., Sanjad, S. A., Rodriguez-Soriano, J., Santos, F., Cremers, C. W., Di Pietro, A., Hoffbrand, B. I., Winiarski, J., Bakkaloglu, A., Ozen, S., Dusunsel, R., Goodyer, P., Hulton, S. A., Wu, D. K., Skvorak, A. B., Morton, C. C., Cunningham, M. J., Jha, V., and Lifton, R. P. (1999) *Nat. Genet.* **21,** 84–90
6. Blair, H. C., Teitelbaum, S. L., Ghiselli, R., and Gluck, S. (1989) *Science* **245,** 855–857
7. Sennoune, S. R., Bakunts, K., Martinez, G. M., Chua-Tuan, J. L., Kebir, Y., Attaya, M. N., and Martinez-Zaguilan, R. (2004) *Am. J. Physiol.* **286,** C1443–C1452
8. Izumi, H., Torigoe, T., Ishiguchi, H., Uramoto, H., Yoshida, Y., Tanabe, M., Ise, T., Murakami, T., Yoshida, T., Nomoto, M., and Kohno, K. (2003) *Cancer Treat. Rev.* **29,** 541–549
9. Farina, C., and Gagliardi, S. (2002) *Curr. Pharm. Des.* **8,** 2033–2048
10. Boyd, M. R., Farina, C., Belfiore, P., Gagliardi, S., Kim, J. W., Hayakawa, Y., Beutler, J. A., McKee, T. C., Bowman, B. J., and Bowman, E. J. (2001) *J. Pharmacol. Exp. Ther.* **297,** 114–120
11. Bowman, E. J., Gustafson, K. R., Bowman, B. J., and Boyd, M. R. (2003) *J. Biol. Chem.* **278,** 44147–44152
12. Beutler, J. A., and McKee, T. C. (2003) *Curr. Med. Chem.* **10,** 787–796
13. Bowman, E. J., Siebers, A., and Altendorf, K. (1988) *Proc. Natl. Acad. Sci. U. S. A.* **85,** 7972–7976
14. Dröse, S., and Altendorf, K. (1997) *J. Exp. Biol.* **200,** 1–8
15. Dröse, S., Bindseil, K. U., Bowman, E. J., Siebers, A., Zeeck, A., and Altendorf, K. (1993) *Biochemistry* (*Mosc.*) **32,** 3902–3906
16. Farina, C., Gagliardi, S., Nadler, G., Morvan, M., Parini, C., Belfiore, P., Visentin, L., and Gowen, M. (2001) *Farmaco* (*Rome*) **56,** 113–116
17. Bowman, B. J., and Bowman, E. J. (2002) *J. Biol. Chem.* **277,** 3965–3972
18. Bowman, E. J., Graham, L. A., Stevens, T. H., and Bowman, B. J. (2004) *J. Biol. Chem.* **279,** 33131–33138
19. Wilkens, S., and Forgac, M. (2001) *J. Biol. Chem.* **276,** 44064–44068
20. Venzke, D., Domgall, I., Kocher, T., Fethiere, J., Fischer, S., and Böttcher, B. (2005) *J. Mol. Biol.* **349,** 659–669
21. Imamura, H., Nakano, M., Noji, H., Muneyuki, E., Ohkuma, S., Yoshida, M., and Yokoyama, K. (2003) *Proc. Natl. Acad. Sci. U. S. A.* **100,** 2312–2315
22. Hirata, T., Iwamoto-Kihara, A., Sun-Wada, G. H., Okajima, T., Wada, Y., and Futai, M. (2003) *J. Biol. Chem.* **278,** 23714–23719
23. Yokoyama, K., and Imamura, H. (2005) *J. Bioenerg. Biomembr.* **37,** 405–410
24. Mandel, M., Moriyama, Y., Hulmes, J. D., Pan, Y. C., Nelson, H., and Nelson, N. (1988) *Proc. Natl. Acad. Sci. U. S. A.* **85,** 5521–5524
25. Meier, T., Polzer, P., Diederichs, K., Welte, W., and Dimroth, P. (2005) *Science* **308,** 659–662
26. Girvin, M. E., Rastogi, V. K., Abildgaard, F., Markley, J. L., and Fillingame, R. H. (1998) *Biochemistry* (*Mosc.*) **37,** 8817–8824
27. Stock, D., Leslie, A. G., and Walker, J. E. (1999) *Science* **286,** 1700–1705
28. Kawasaki-Nishi, S., Nishi, T., and Forgac, M. (2003) *J. Biol. Chem.* **278,** 41908–41913
29. Harrison, M. A., Murray, J., Powell, B., Kim, Y. I., Finbow, M. E., and Findlay, J. B. (1999) *J. Biol. Chem.* **274,** 25461–25470
30. Harrison, M., Powell, B., Finbow, M. E., and Findlay, J. B. (2000) *Biochemistry* (*Mosc.*) **39,** 7531–7537
31. Harrison, M., Durose, L., Song, C. F., Barratt, E., Trinick, J., Jones, R., and Findlay, J. B. (2003) *J. Bioenerg. Biomembr.* **35,** 337–345
32. Murata, T., Yamato, I., Kakinuma, Y., Leslie, A. G., and Walker, J. E. (2005) *Science* **308,** 654–659
33. Bowman, E. J., and Bowman, B. J. (1997) in *Biomembranes* (Packer, L., and Fleischer, S., eds) pp. 861–872, Academic Press, San Diego
34. Davis, R. H. (2000) *Neurospora: Contributions of a Model Organism*, pp. 273–303, Oxford University Press, New York
35. Vogel, H. J. (1964) *Am. Nat.* **98,** 435–446
36. Bowman, E. J., Kendle, R., and Bowman, B. J. (2000) *J. Biol. Chem.* **275,** 167–176
37. Sachs, M. S., Selker, E. U., Lin, B., Roberts, C. J., Luo, Z., Vaught-Alexander, D., and Margolin, B. S. (1997) *Nucleic Acids Res.* **25,** 2389–2395
38. Chavez, C., Bowman, E. J., Reidling, J. C., Haw, K. H., and Bowman, B. J. (2006) *J. Biol. Chem.* **281,** 27052–27062
39. Margolin, B. S., Freitag, M., and Selker, E. U. (1997) *Fungal Genet. Newsl.* **44,** 34–36
40. McLachlan, A. D. (1982) *Acta Crystallogr. Sect. A* **38**, 871–873
41. Rohl, C. A., Strauss, C. E., Misura, K. M., and Baker, D. (2004) *Methods Enzymol.* **383,** 66–93
42. Sayle, R. A., and Milner-White, E. J. (1995) *Trends Biochem. Sci.* **20,** 374
43. John, U. P., and Nagley, P. (1986) *FEBS Lett.* **207,** 79–83
44. Kawasaki-Nishi, S., Nishi, T., and Forgac, M. (2001) *Proc. Natl. Acad. Sci. U. S. A.* **98,** 12397–12402
45. Deleted in proof
46. Baker, G. H., Brown, P. J., Dorgan, R. J. J., Everett, J. R., Ley, S. V., Slawin, A. M. Z., and Williams, D. J. (1987) *Tetrahedron Lett.* **28,** 5565–5568
47. Wang, Y., Inoue, T., and Forgac, M. (2005) *J. Biol. Chem.* **280,** 40481–40488
48. Whyteside, G., Meek, P. J., Ball, S. K., Dixon, N., Finbow, M. E., Kee, T. P., Findlay, J. B., and Harrison, M. A. (2005) *Biochemistry* (*Mosc.*) **44,** 15024–15031
49. Arai, H., Terres, G., Pink, S., and Forgac, M. (1988) *J. Biol. Chem.* **263,** 8796–8802
50. Murata, T., Arechaga, I., Fearnley, I. M., Kakinuma, Y., Yamato, I., and Walker, J. E. (2003) *J. Biol. Chem.* **278,** 21162–21167
51. Sebald, W., Graf, T., and Lukins, H. B. (1979) *Eur. J. Biochem.* **93,** 587–599
52. Sigrist-Nelson, K., Sigrist, H., and Azzi, A. (1978) *Eur. J. Biochem.* **92,** 9–14
53. Foster, D. L., and Fillingame, R. H. (1982) *J. Biol. Chem.* **257,** 2009–2015
54. Iwata, M., Imamura, H., Stambouli, E., Ikeda, C., Tamakoshi, M., Nagata, K., Makyio, H., Hankamer, B., Barber, J., Yoshida, M., Yokoyama, K., and Iwata, S. (2004) *Proc. Natl. Acad. Sci. U. S. A.* **101,** 59–64
55. Melnik, V. I., and Bowman, B. J. (1996) *Biochim. Biophys. Acta* **1273,** 77–83
56. Hirata, R., Graham, L. A., Takatsuki, A., Stevens, T. H., and Anraku, Y. (1997) *J. Biol. Chem.* **272,** 4795–4803
57. Huss, M., Ingenhorst, G., Konig, S., Gassel, M., Dröse, S., Zeeck, A., Altendorf, K., and Wieczorek, H. (2002) *J. Biol. Chem.* **277,** 40544–40548
58. Nakai, H., and Matsutani, S. (1992) *Acta Crystallogr. Sect. C Cryst. Struct. Commun.* **48**, 1519–1521